

Heteroepitaxy of lattice-matched compound semiconductors on silicon

Klaus J. Bachmann

Department of Materials Science and Engineering and Department of Chemical Engineering, North Carolina State University, Raleigh, North Carolina 27695-7919

Nikolaus Dietz, Amy E. Miller, David Venables, and James T. Kelliher

Department of Materials Science and Engineering, North Carolina State University, Raleigh, North Carolina 27695-7919

(Received 24 October 1994; accepted 13 February 1995)

The heteroepitaxial overgrowth of silicon by nearly lattice-matched compound semiconductors is reviewed in the context of the separation of the chemical problems associated with the initial sealing of the silicon surface by a contiguous epitaxial compound film from the problems associated with the generation of strain during heteroepitaxial growth. Of the mixed compound systems available dilute solid solutions of composition $\text{Al}_x\text{Ga}_{1-x}\text{N}_y\text{P}_{1-y}$ and $\text{ZnS}_y\text{Se}_{1-y}$ as well as $\text{ZnSi}_x\text{Ge}_{1-x}\text{P}$ are suitable candidates for the exactly lattice-matched epitaxial overgrowth of silicon. Real-time process monitoring by nonintrusive methods is important for gaining an understanding of the epitaxial overgrowth mechanism and for controlling the film properties. A new method, *p*-polarized reflectance spectroscopy is introduced that provides detailed information about the growth rate per cycle, the bulk optical properties of the film and its topography. Submonolayer resolution is accomplished for thousands of Å of film growth by pulsed chemical beam epitaxy. While the cubic materials considered here generally afford easier control of the electrical and optical properties, the noncubic materials have advantages in the sealing of the silicon surface because of their anisotropic growth and the formation of metastable solid solutions that may permit the graded growth of compound films under exactly lattice-matched conditions. Therefore, no clear-cut preference in the materials selection for nearly lattice-matched overgrowth of silicon by compound semiconductors can be identified at this time. © 1995 American Vacuum Society.

I. INTRODUCTION

Silicon is a unique substrate because of its exceptional perfection, purity, and low cost. It provides a reliable basis for the manufacturing of integrated circuits supporting a multibillion dollar industry. Therefore, attempts at extending the use of silicon substrates through the provision of high quality heteroepitaxial coatings to other applications that require the use of compound semiconductors represent a valid goal of advanced materials engineering. In particular, the integration of silicon and compound semiconductor devices is of interest in the context of future advanced microelectronic circuits, e.g., vertically integrated circuits, optically interconnected common memory, and integrated sensor circuits.

The primary obstacle to the commercial use of silicon-based heterostructures is the formation of defects that limit the performance and reliability of devices and circuits. There are two distinct albeit interacting sources of defect formation: (1) lattice strain and (2) chemical incompatibilities in the early stages of heteroepitaxial overgrowth. Generally, the properties required for the optimization of specific devices are not realized in compounds that lattice-match silicon exactly. This has stimulated attempts at the direct growth of lattice-mismatched compounds on silicon substrates (e.g., GaAs/Si and ZnSe/Si heterostructures^{1,2}). Experience has shown that attempts at understanding and controlling the complex synergism of chemical interactions and strain-induced defect formation under the conditions of strained overgrowth of silicon by mismatched compound semiconductors is a forbiddingly difficult task. Therefore, we consider it advantageous to grow first a buffer layer of a lattice-

matched compound that seals the silicon surface, which is followed by the deposition of an appropriately graded layer of the desired lattice-mismatched compound, having the same crystal structure and similar chemical composition as the buffer layer. The control of the problems associated with the interfacial chemistry thus are separated from the control of strain induced defect formation. That this strategy works has been demonstrated recently for well-engineered III-V/Si heterostructures.³

The key issue in the epitaxial overgrowth of silicon by a nearly lattice-matched compound is the control of planar defect formation during the initial period of nucleation and overgrowth. This is demonstrated by Fig. 1, which shows a cross sectional transmission electron microscopy (TEM) image of a GaP film on Si(001) grown by chemical beam epitaxy. Even though GaP is nearly lattice-matched to silicon, the planar defects in the heterostructure have similar spacings as expected between the misfit dislocation for the most important lattice-mismatched compound semiconductor heterostructures, e.g., GaAs/Si or ZnSe/Si. Since for nearly lattice-matched heterostructures, grown by a low temperature process, strain cannot be the cause of the observed defect formation, it must be related to the chemical interactions on the Si surface in the very early stages of epitaxial overgrowth. Real-time process monitoring is essential for developing an understanding of the nature of these interactions without which no progress is possible with regard to the engineering of the defect propagation in lattice-mismatched heterostructures on lattice-matched interlayers on a silicon substrate.

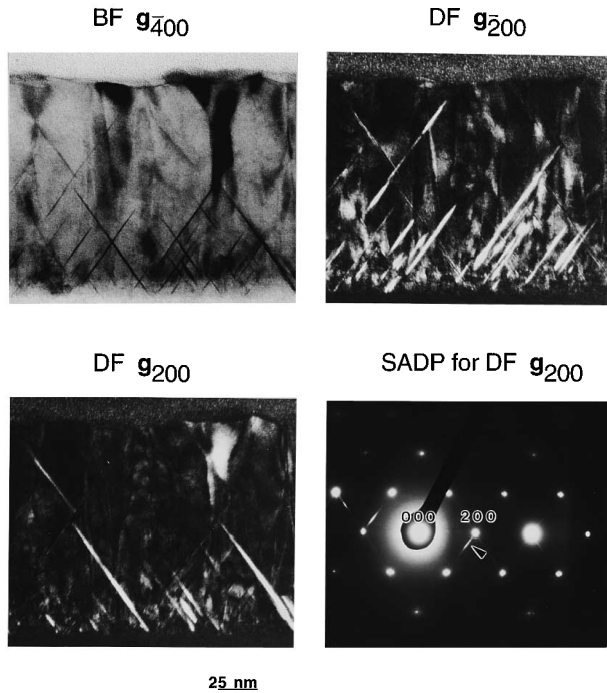


FIG. 1. Bright field (top left) and dark field (top right and bottom left) cross sectional transmission electron microscopy images of GaP epilayers on Si(001). Bottom right: selected area diffraction pattern.

In this article, we first review the choices of materials that are available for nearly lattice-matched heteroepitaxy on silicon and then focus on a specific epitaxial method, pulsed chemical beam epitaxial (PCBE), and a specific heterostruc-

ture, GaP/Si(001), to introduce a new method of real-time process monitoring, *p*-polarized reflectance spectroscopy (PRS), which accomplishes the characterization of the growth process with Å resolution over thousands of Å of film growth.^{4,5} The article concludes with an outlook at chalcopyrite structure compounds and alloys that lattice-match silicon and that are of interest in the context of nonlinear optical applications.

II. MATERIALS SELECTION

Figure 2 shows a plot of the band gaps and equivalent lattice parameters for a selection of semiconductors. Of the III–V compounds, GaP and AlP provide for the closest matching of the lattice constants to silicon, that is, $\sim 0.36\%$ at room temperature. In view of the substantial differences of the coefficients of thermal expansion between these compounds and silicon, the minimization of strain effects under the conditions of heteroepitaxial growth mandates the selection of low temperature processing. This is possible, for example, by molecular beam epitaxy (MBE)³ or chemical beam epitaxy (CBE)⁶ and is further reinforced by the low thermal budget requirement of modern single wafer silicon processing.

Of the II–VI compounds ZnS lattice matches silicon within 0.39% at room temperature and is thus a suitable candidate for the provision of nearly lattice-matched interlayers on silicon. In view of their highly anisotropic growth, hexagonal II–VI compounds provide for a greater tendency of the nuclei to spread across the silicon surface than attainable with cubic materials, particularly on the {111} surface. Also,

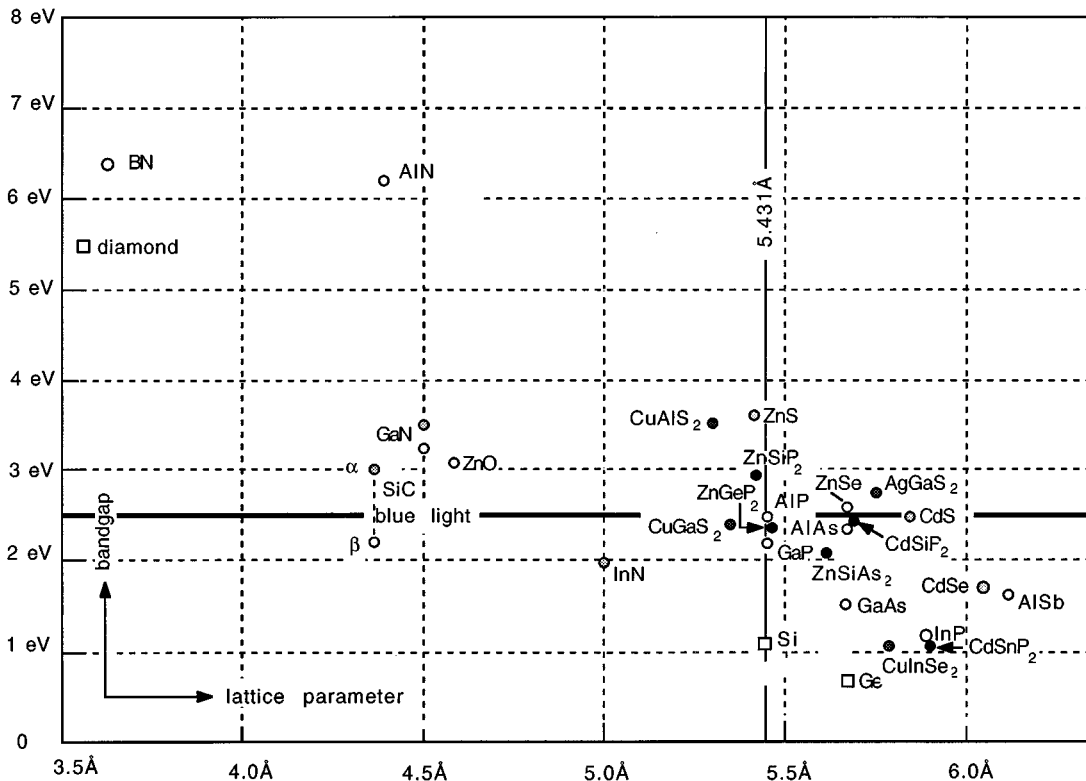


FIG. 2. Bandgaps vs equivalent lattice parameters for selected compounds.

chalcogenides and pnictides that crystallized in layer structures with weak van der Waals bonds between the layers may be useful choices for the smooth overgrowth of silicon surfaces, accommodating residual strain parallel to the interface and providing a good chemical match to the II–VI and III–V compounds. However, the reliability of circuits incorporating layer compounds may be compromised both by their chemistry and the weak bonding of the layers.

There exist a number of ternary and quaternary III–V and II–VI systems, where the lattice parameters of the constituent binary compounds straddle the lattice parameter of silicon. This has led to the prediction of exactly lattice-matched alloys for heteroepitaxial growth on silicon, e.g., in the GaN–GaAs system.⁷ However, built-in strain restricts the existence ranges of solid solutions in thermodynamic equilibrium, so that only a limited number of realistic choices of exactly lattice-matched solid solutions emerge from the large number of pseudoternary and pseudoquaternary systems containing hypothetical compositions that match the lattice parameter of silicon on the basis of Vegard's law. Opportunities for the engineering of exactly lattice-matched epilayers in strongly lattice-mismatched multinary systems exist only if at least one component compound nearly lattice-matches silicon.

For example, in the AlN–GaN–AlP–GaP system for which wide regions of immiscibility in solid state are expected, a region of relatively small built-in strain exists close to the $\text{Al}_x\text{Ga}_{1-x}\text{P}$ pseudobinary. Critical temperatures well above the liquidus surface have been predicted by the delta lattice parameter (DLP) model on the GaN–GaP pseudobinary.⁸ The nitrogen concentrations required to achieve exact lattice matching to silicon at room temperature are small, $y=0.0196$ and 0.0189 on the $\text{GaN}_y\text{P}_{1-y}$ and $\text{AlN}_y\text{P}_{1-y}$ pseudobinaries, respectively. This is above the solid solubility of nitrogen in GaP.⁹ However, access to metastable solid solutions at low growth temperatures is likely to extend the existence range of solid solutions over a limited range of solid solutions in the vicinity of the AlP–GaP pseudobinary. Therefore, in our opinion, dilute $\text{Al}_x\text{Ga}_{1-x}\text{N}_y\text{P}_{1-y}$ solid solutions should represent a possibility for the realization of exactly lattice-matched III–V/silicon heterostructures.

In addition to the III–V and II–VI compounds, there exist two classes of tetrahedrally coordinated compounds that crystallize in the chalcopyrite structure, which is derived from the zincblende structure by ordered cation substitution. Substituting the group III sublattice of the III–V compounds at 1:1 ratio by group II and group IV atoms results in the II–IV–V₂ compounds and substituting the group II sublattice of the II–VI compounds at 1:1 ratio by group I and group III atoms results in the I–III–VI₂ compounds. None of the I–III–VI₂ compounds are close enough in their *a*-axis lattice parameters to the lattice constant of silicon to qualify as suitable choices. The II–IV–V₂ compounds ZnGeP₂ and ZnSiP₂ lattice match silicon on the (001) interface within +0.4% and –0.6%, respectively. Since the pseudobinary ZnSi_xGe_{1-x}P₂ system spans only a small range of lattice parameters that straddle the lattice parameter of Si, the quaternary solid solution ZnSi_{0.47}Ge_{0.53}P₂ that lattice matches silicon exactly should be accessible. Also we have shown

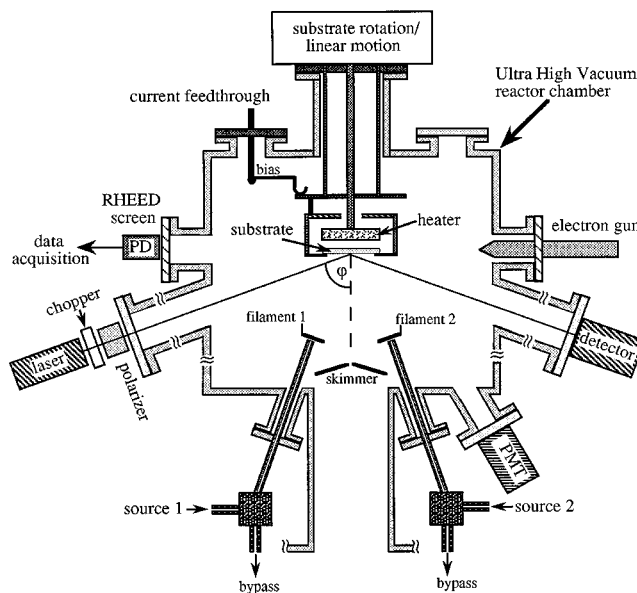


FIG. 3. Schematic representation of a system for pulsed chemical beam epitaxy of III–V compounds and alloys, incorporating provisions for real-time monitoring by *p*-polarized reflectance spectroscopy and RHEED.

that extended ranges of metastable solid solutions exist in the ZnSiP₂–ZnGeP₂–Si–Ge system, which could serve as the basis for graded exactly lattice-matched growth of II–IV–V₂ alloys on silicon.¹⁰

III. PULSED CHEMICAL BEAM EPITAXY OF GaP ON Si(001)

Although opportunities for exactly lattice-matched growth exist among the ZnS based II–VI alloys, we focus in our work on pnictides. This preference is predicated in part by preliminary studies of the interdiffusion of phosphorus and gallium at the interfaces of Si/GaP/Si double heterostructures upon rapid thermal annealing (RTA). They show that GaP/Si heterostructures are stable with regard to interdiffusion under the conditions of ultra-large-scale integration (ULSI) processing that requires high temperature rapid thermal annealing (RTA) steps in late stages of the processing sequence.

Figure 3 shows a schematic representation of a cut through a chemical beam epitaxy chamber. The substrate points downward and is radiatively heated from its back side. The gas source beams, triethylgallium (TEG) and tertiary-butylphosphine (TBP), are brought into the chamber via three-way valves, so that they can be pulsed with computer-controlled delay between the individual pulses. Also, a beam of hydrogen is provided to assist the removal of organic radicals from the surface of the growing film. Prior to insertion into the process chamber via the loadlock, the silicon substrate wafers receive an RCA clean followed by etching in buffered HF to create a hydrogen-terminated (001) surface of 1×1 reconstruction. The substrates are heated in the presence of both TBP and hydrogen beams to the growth temperature. Then the switching cycles are initiated to start pulsed CBE of GaP. Previously reported research established a process window between 260 and 410 °C, where the growth rate is a weak function of temperature.⁶ Most of the growth reported here is carried out at 350 °C.

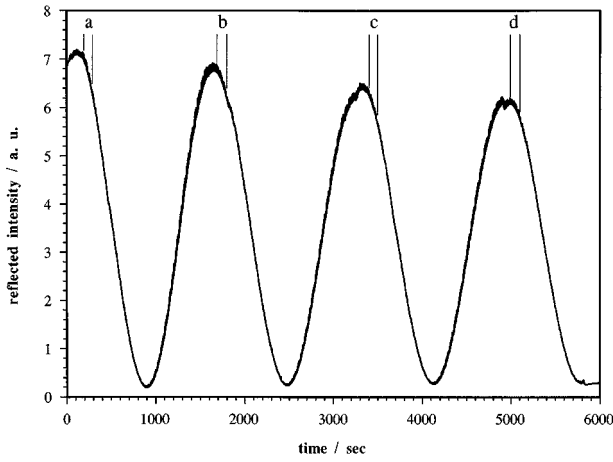


FIG. 4. Quarter-wavelength oscillations in the intensity of the p -polarized reflected beam for the epitaxial growth of GaP on Si(001) at 350 °C using t -butPH₂ and Ga(C₂H₅)₃ source beams. The distance between adjacent minima corresponds to a GaP film thickness of 1750±50 Å.

In order to gain a better understanding and control of the heteroepitaxial process, provisions are made for real-time monitoring of the initial surface cleanliness/structure and the film growth by PRS. PRS is based on the changes in the reflectance of the heteroepitaxial stack during its formation with regard to a beam of p -polarized light that impinges onto the surface at the Brewster angle of the substrate. In this work we employed a combination of a HeNe laser and a Glan–Thompson polarizer to generate a p -polarized beam of 632.8 nm wavelength at which the GaP is transparent. The reflected beam is detected by a photodiode, processed through a phase sensitive amplifier, and read into a computer. In addition, the radiation that is scattered by the growing film into the entrance slit of a photomultiplier is detected at a location well removed from the plane of incidence of the impinging light beam. It provides information on the roughness of the top and bottom interfaces of the film.

The complex reflectivity of a three-layer stack composed of materials labeled 0, 1, and 2 with interfaces labeled 01 and 12, respectively, is given by

$$rr_p = \frac{r_{01p} + r_{12p} \exp(-2i\Phi)}{1 + r_{01p}r_{12p} \exp(-2i\Phi)}, \quad (1)$$

with reflectivity coefficients

$$r_{01p} = \frac{\epsilon_f \cos \varphi_0 - \sqrt{\epsilon_a} \sqrt{\epsilon_f - \epsilon_a} \sin^2 \varphi_0}{\epsilon_f \cos \varphi_0 + \sqrt{\epsilon_a} \sqrt{\epsilon_f - \epsilon_a} \sin^2 \varphi_0}, \quad (2)$$

$$r_{12p} = \frac{\epsilon_s \sqrt{\epsilon_f - \epsilon_a} \sin^2 \varphi_0 - \epsilon_f \sqrt{\epsilon_s - \epsilon_a} \sin^2 \varphi_0}{\epsilon_s \sqrt{\epsilon_f - \epsilon_a} \sin^2 \varphi_0 + \epsilon_f \sqrt{\epsilon_s - \epsilon_a} \sin^2 \varphi_0}, \quad (3)$$

and phase

$$\Phi = \frac{2\pi t_f}{\lambda} \sqrt{\epsilon_f - \epsilon_a} \sin^2 \varphi_0. \quad (4)$$

Upon initiation of heteroepitaxial growth, the reflected intensity $R_p = rr_p rr_p^*$ oscillates with a period corresponding to a quarter-wavelength between adjacent minima as illustrated in Fig. 4, providing information on the growth rate and on

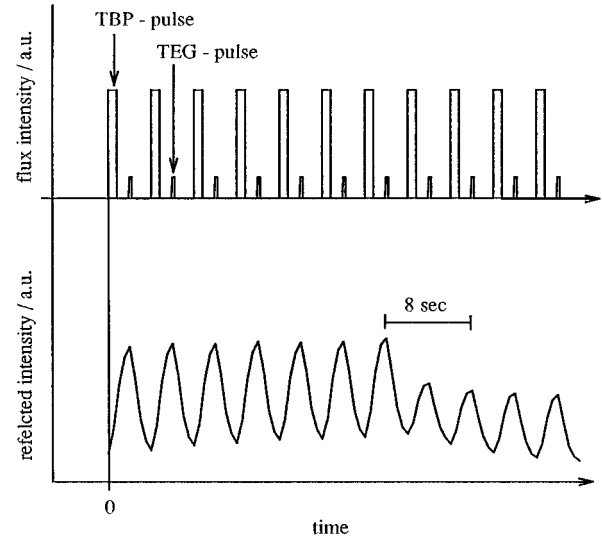


FIG. 5. Relation between the fine structure in the intensity of the p -polarized reflected beam and the precursor pulse sequence under the conditions of PCBE of GaP at 350 °C using t -butPH₂ and Ga(C₂H₅)₃ source beams.

the optical properties of the growing film.¹¹ Note that contamination of the surface by interactions with a contaminated residual vapor atmosphere during heating to the growth temperature would present itself by changes in the dielectric properties that could be detected early. The monitoring of the surface properties prior to growth thus provides valuable information with regard to the reproducible initial conditions for the growth process and the opportunity for termination at an early stage in the event of contamination problems.

Detailed information regarding the nucleation and epitaxial overgrowth process is gained from the analysis of the fine structure that is superimposed on the quarter-wavelength oscillations of the reflected intensity. It relates to modifications of the dielectric function in the vicinity of the surface of the evolving heteroepitaxial layer due to the exposure to the sequential Ga(C₂H₅)₃ and t -butPH₂ pulses. Figure 5 shows the correlation of the fine structure to the chemical changes on the surface. Each peak in the fine structure represents a complete precursor cycle. In contrast to reflection high-energy electron diffraction (RHEED) oscillations, the fine structure is maintained for thousands of cycles as illustrated in Fig. 6. Thus PRS permits to follow the heteroepitaxial growth process with submonolayer resolution over thousands of monolayers, thus providing access to the study of the growth mechanism in both the nucleation and initial overgrowth phase as well as in the later stages of film growth. In the case of homoepitaxy, the quarter-wavelength oscillations in the reflected intensity do not exist, but the fine structure persists. It is similar to the surface photoabsorption (SPA) previously described in the context of GaAs homoepitaxial structures made by MBE.¹² However, a difference exists between SPA and PRS in that SPA chooses a laser energy above the absorption edge to obtain high surface sensitivity, while PRS works at below bandgap energy to probe for both bulk and surface effects. The latter permits a calibration of the layer thickness deposited per precursor cycle on the basis of the quarter wavelength oscillations observed in heteroepitaxial

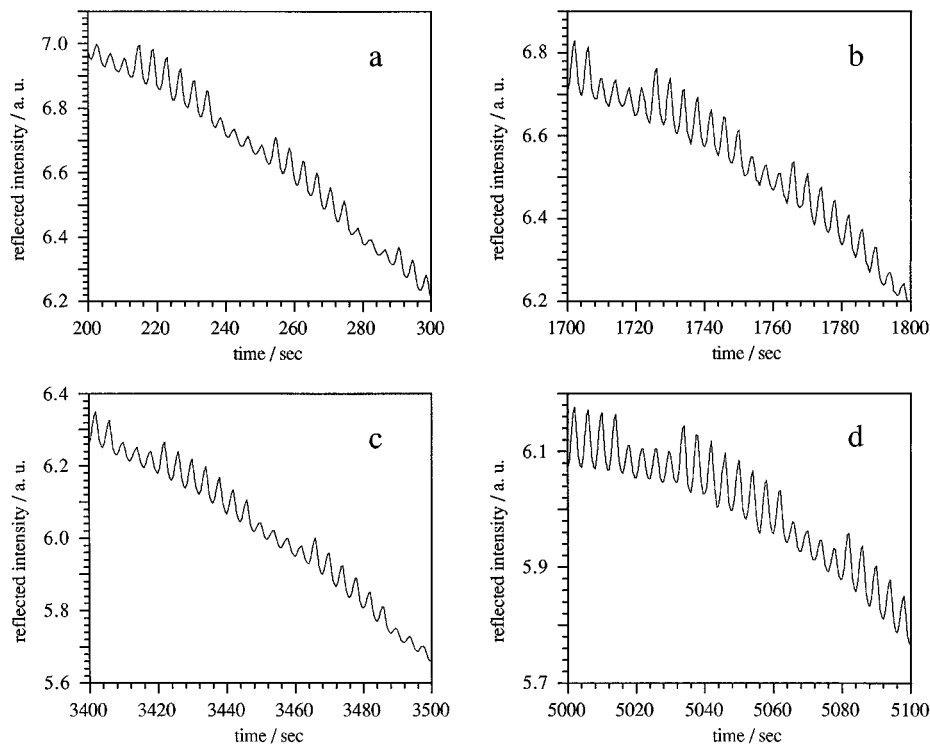


FIG. 6. Selected portions of the fine structure in the intensity of the *p*-polarized reflected beam recorded at time intervals labeled a, b, c, and d in Fig. 4.

growth experiments. In the case of GaP epitaxy on Si(001) by PCBE the layer thickness deposited per precursor cycle does not change from the initial overgrowth phase till the end of the film growth depicted in Fig. 4.

Without precautions in the selection of the source compound pulse heights, widths, and delays, the fine structure signal is amplitude modulated with a period that persists over extended periods of film growth, but undergoes slow changes as the thick film heterostructure evolves from the initial overgrowth phase, as illustrated in Fig. 5. In the special case of homoepitaxy of GaP on GaP(001) substrates, the periodicity in the amplitude modulation of the fine structure coincides with a similar modulation of the amplitude of the scattered radiation.⁴ Therefore, it is at least in part related to the surface roughness that undergoes a slow change in the course of thick film depositions. In addition to possible periodic variations in the surface topography, chemical changes in the effective dielectric function contribute to the amplitude modulation of the fine structure, which may be eliminated by an appropriate choice in the relative width, amplitude, and delay of the precursor pulses. PRS provides thus a means for real-time tuning of the deposition conditions of PCBE toward atomic layer epitaxy (ALE). An unequivocal check for self-terminating ALE mechanisms that should result in monolayer thickness per cycle independent of the amplitude and width of the precursor pulses is given by the possibility of calculating the layer thickness per pulse sequence from the observed PRS signal. Under the conditions of PCBE of GaP on Si for the precursor chemistry chosen by us self-terminating ALE does not exist.

Figures 7(a) and 7(b) show atomic force microscopy (AFM) images (left) and line scans (right) just after sealing

of the silicon (001) surface by a contiguous GaP film and after 4455 Å GaP deposition. The root-mean-square (rms) surface roughness changes from 1 nm for Fig. 7(a) to 2.26 nm after an extended period of growth. Note that the AFM line scans cover a wider area than shown in the images. A complete evaluation at different length scales is still outstanding.

Figures 8(a) and 8(b) show equivalent AFM images and line scans for the silicon (001) substrate prior to growth and after five precursor cycles, respectively. The rms surface roughness prior to growth and after nucleation of GaP is 0.5 and 1.9 nm, respectively, that is, the surface after nucleation is substantially rougher than after sealing of the silicon surface by a contiguous layer of GaP.

Although the image of the nuclei spreading over the silicon surface seems to reveal slanted side faces, the actual habit of the nuclei is flatter than suggested by the image, that is, the spikes in the line scan are typically 10 nm high and 80 nm across. This height scale is consistent within the error limits with the habit calculated from the growth rate per cycle (~ 3 Å) and the surface coverage after five cycles ($\sim 20\%$). The GaP nuclei on Si(001) thus tend to grow out into three-dimensional islands, which is due to two independent causes: (i) the thermodynamic definition of the habit of the nuclei by the modified Wulff's law¹³ and (ii) the catalytic enhancement of the pyrolysis of *t*-butylphosphine on the surface of the GaP nuclei as compared to the bare Si surface. This explains the differences in the growth kinetics prior and after sealing of the silicon surface. Inhomogeneous growth conditions that are caused by the different catalytic properties of the coexisting GaP and Si surface elements prevail during the initial nucleation and overgrowth stage, so that

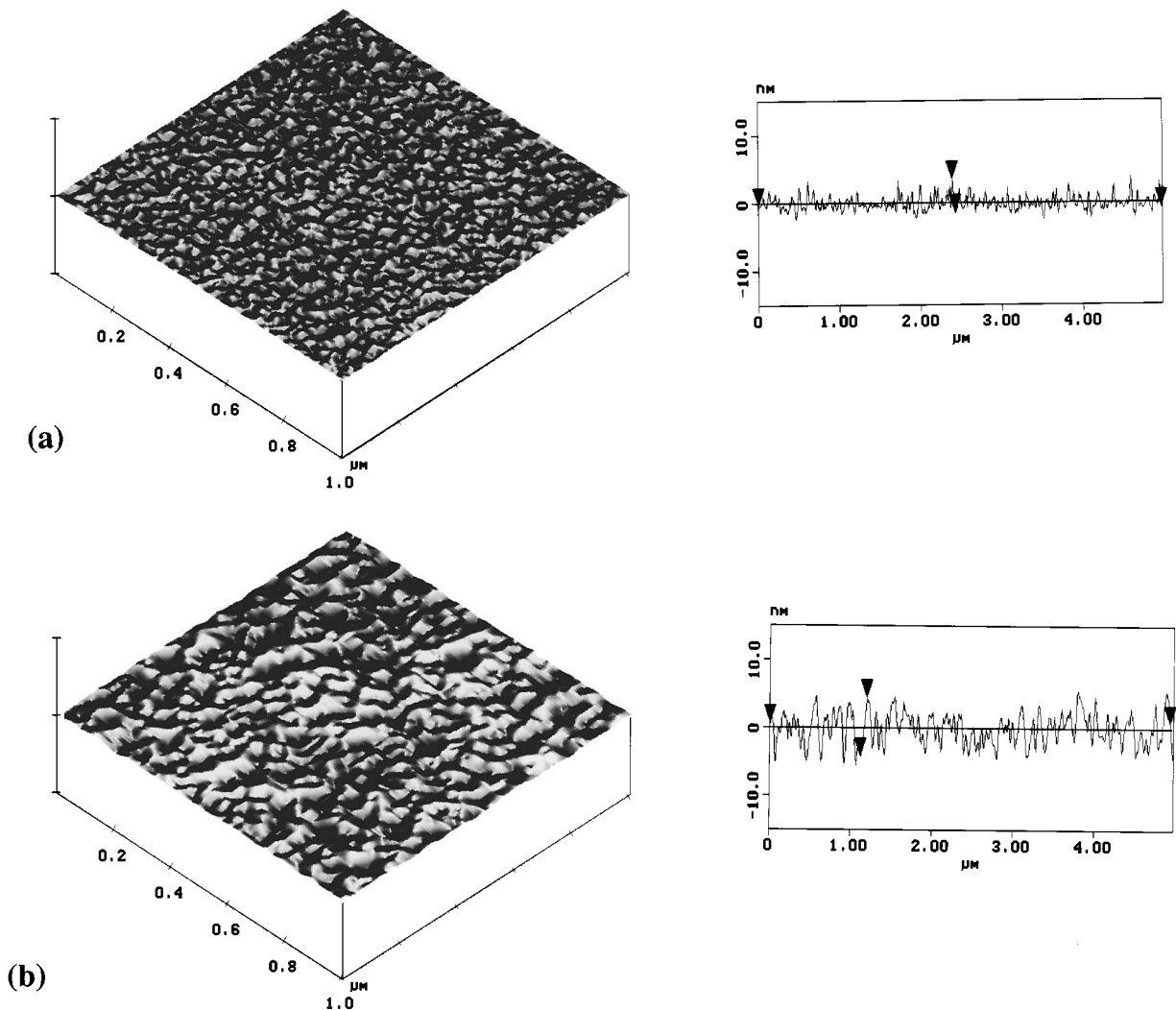


FIG. 7. AFM images (left) and line scans (right) of (a) a Si(001) surface at the stage of complete sealing by a contiguous GaP epilayer corresponding to an exposure to ten precursor cycles, and (b) the surface of the same wafer after exposure to 1485 precursor cycles corresponding to a GaP epilayer thickness of ~ 4455 Å.

even at uniform incident fluxes of *t*-butPH₂ and Ga(C₂H₅)₃ the surface coverages by Ga and P precursors to growth on the GaP islands relative to the remaining bare silicon surface areas differ. This complication vanishes as soon as the silicon surface is overgrown by a contiguous GaP epilayer.

Additional insight into the nucleation process is obtained from the analysis of the PRS intensity in the initial period of heteroepitaxial overgrowth. The corrugation in the surface during this stage of film growth is incorporated into the description of the reflectivity by replacing the dielectric function of the bulk film by an effective dielectric function

$$\epsilon_{\text{eff}} = \epsilon_a \frac{\epsilon_f(1+2q) + 2\epsilon_a(1-q)}{\epsilon_f(1-q) + \epsilon_a(2+q)}, \quad (5)$$

that varies for a range of the corrugation parameter $0 \leq q \leq 1$ between the dielectric functions of the ambient ($q=0$) and the compact film ($q=1$). Thus the effective dielectric function of a corrugated GaP film that covers the silicon surface incompletely is expected to be substantially smaller than the dielectric function for a contiguous film. Because of the larger difference between the dielectric constants of the sub-

strate and the corrugated film, this should express itself in an enhanced PRS intensity during the nucleation period depending on the degree of deviation from two-dimensional growth. Indeed, we have observed in specific cases substantial enhancements in both the reflected and scattered intensities during the nucleation period. Figure 9(a) shows this for conditions, where AFM images and line scans—taken at selected intervals in the initial period of nucleation and heteroepitaxial overgrowth—reveal the formation of three-dimensional islands resulting in $\sim 20\%$ coverage after five precursor cycles and complete coverage after ten cycles. Figure 9(b) shows a magnified view of the PRS intensity for the experiment shown in Fig. 4 during the initial period of nucleation and overgrowth. Here no substantial enhancements of the signal are observed, suggesting a nearly two-dimensional nucleation and overgrowth mechanism. Unfortunately, this is not always observed, which we relate tentatively to irreproducible cleanliness and structure of the silicon surface.

We have shown previously that the CBE growth of GaP on Si(001) and Si(111) surfaces proceeds highly selectively with regard to surface areas masked by SiO₂ or SiC.¹⁴ Al-

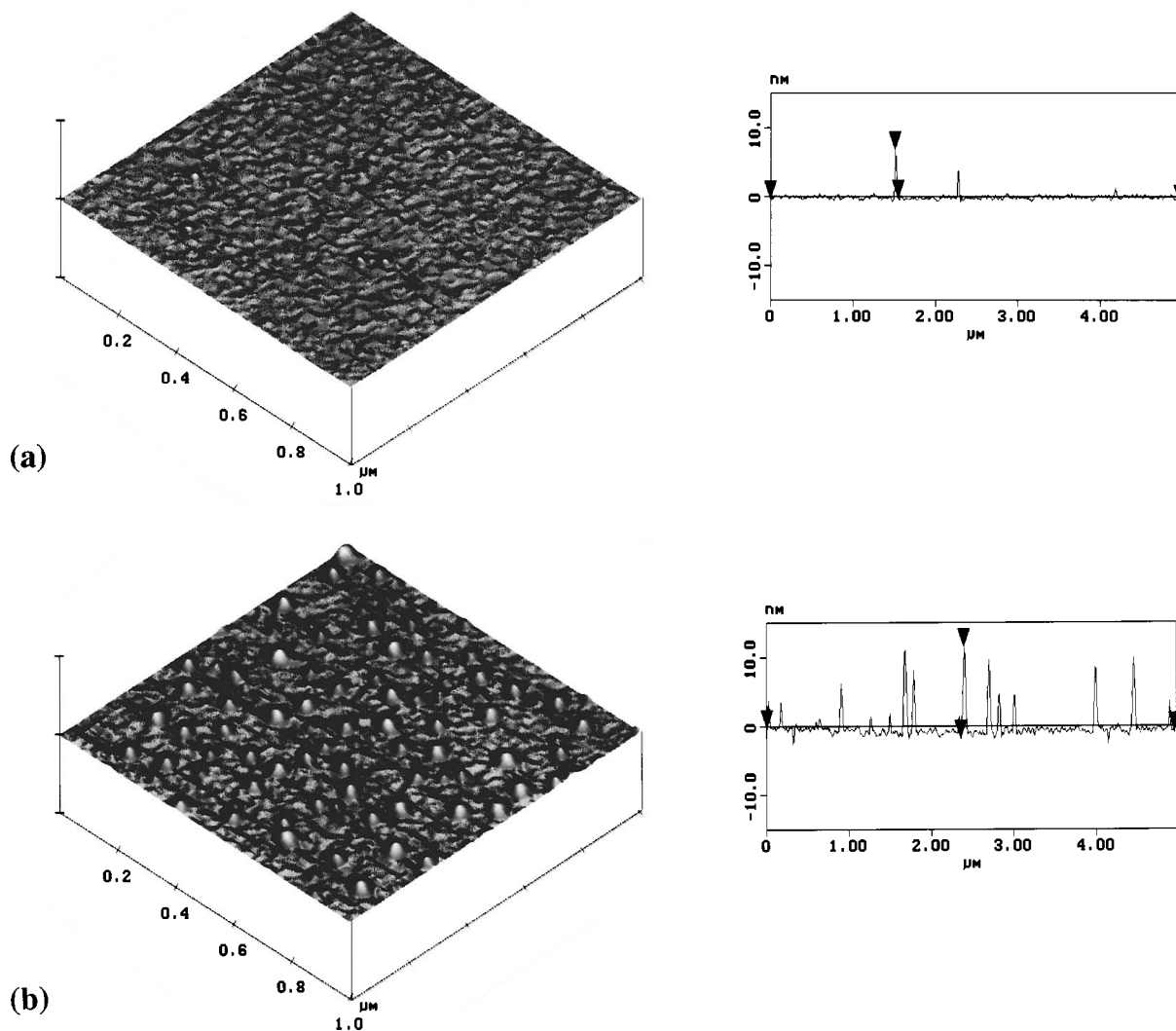


FIG. 8. AFM images (left) and line scans (right) of (a) a clean hydrogen terminated Si(001) surface prior to heating and (b) a Si(001) surface after exposure to five precursor cycles.

though this is a desirable feature in the context of ULSI processing, problems must be expected under the conditions of forced heteroepitaxial overgrowth of the silicon surface by GaP nuclei in surface areas that are contaminated by residual oxygen and other contaminants. A driving force for the nucleation of planar defects is provided on the basis of the Gillespie–Nyholm principle¹⁵ by the repulsive interactions between the lone pairs of electrons on the group V or group VI precursors to the growth of III–V or II–VI epilayers on the one side and the lone pairs of electrons on the oxygen atoms of residual oxide patches on the other side. At the boundary between the {111} facet on a III–V or II–VI nucleus sweeping over the Si surface and a patch of oxygen atoms on the silicon surface the group V or group IV precursors to growth thus may be forced to settle into faulted surface positions that maximize the distance between the surface oxygen and group V or group VI atoms.

There are several observations reported in the literature that support this interpretation. For example, in the epitaxial overgrowth of Si by ZnSe, the formation of planar defects is significantly reduced upon use of an arsine preflow that terminates the silicon (001) surface by arsenic atoms, which

prevent further interactions between the surface and incoming Se precursors to growth.¹⁶ Also, a substantial improvement of GaP epitaxy on Si based on As termination of the Si surface by arsine preflow during heating and high temperature annealing, as well as on cooling from the annealing to the process temperature in an arsine blanket, has been reported.¹⁷ Furthermore, we have observed that the provision of a hydrogen beam that scavenges both oxygen containing molecules of the residual gas atmosphere and carbon containing radicals at the surface of the GaP film is an effective means for reducing the density of planar defects under the conditions of PCBE.¹⁸ Since a very small coverage of the silicon surface by contaminants that is difficult to detect ($\Theta \leq 10^{-4}$) suffices to initiate the nucleation of planar defects in the epitaxial film at a density that prohibits its use for device fabrication, future improvements in the control of planar defect formation will probably continue to rely on empirical improvements of the surface cleanliness (e.g., by switching from the conditions of homoepitaxial Si deposition to heteroepitaxial GaP growth). In addition to the control of the surface cleanliness, also the control of the initial surface topography will be important to optimize the complicated

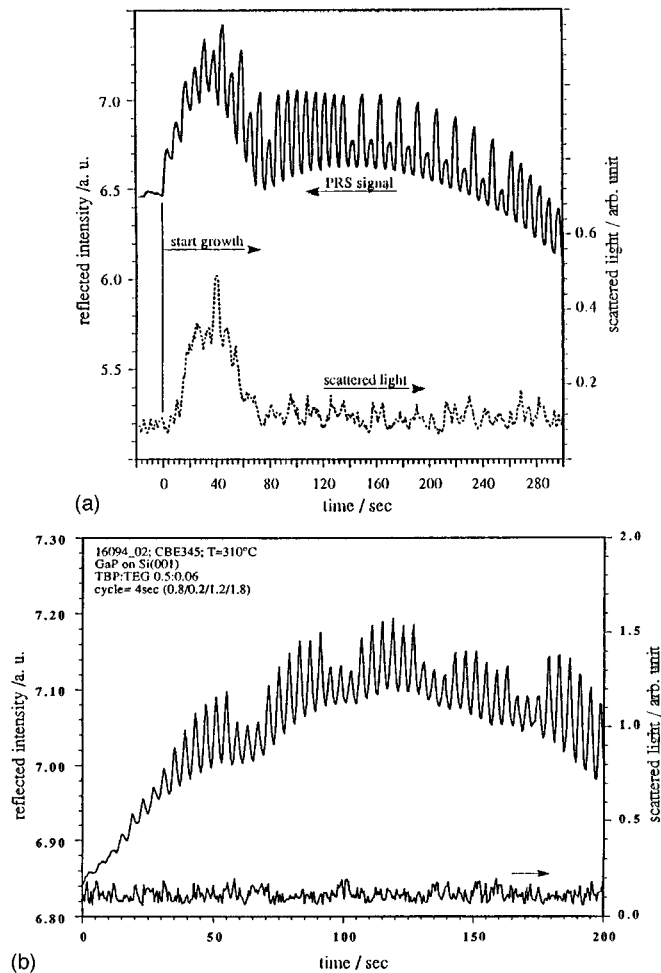


Fig. 9. Fine structure in the PRS intensity during the initial overgrowth stage for (a) conditions resulting in three-dimensional nucleation and overgrowth and (b) the same growth experiment as used in Figs. 4 and 6.

step flow under the conditions of PCBE at low substrate temperatures, where nucleation on terraces between existing steps plays an important role.

IV. HETEROEPITAXY OF NONCUBIC LATTICE-MATCHED COMPOUNDS ON SILICON

Since the $\text{ZnSiP}_2\text{-ZnGeP}_2$ system exhibits small changes in the lattice parameter with composition and matches the lattice constant of Si at $x=0.53$, it is of interest in the context of exactly lattice-matched growth on Si substrates. Smooth heteroepitaxial films of ZnGeP_2 are obtained by organometallic chemical vapor deposition at atmospheric pressure at 585°C on GaP and Si substrates, respectively.^{19,20} Also, epitaxial films of $\text{ZnSi}_x\text{Ge}_{1-x}\text{P}$ have been produced by organometallic chemical vapor deposition (OMCVD) at the same substrate temperature.²¹

The key question that will be decisive for the viability of $\text{ZnSi}_x\text{Ge}_{1-x}\text{P}_2$ heterostructures in nonlinear optics and integrated optics applications is as to whether or not low temperature chemical vapor deposition (CVD) processes provide for sufficient control of the point defect chemistry in this material, which is more complex than for binary compounds and their alloys. Under the conditions of high temperature

processing, e.g., crystal growth from the melt, disorder on the cation sublattice is quenched-in upon cooling to room temperature. Two broad bands of deep donors ($D1$) and acceptors ($A1$) are associated with this disorder and dominate the residual absorption in the near infrared.²²

The density of filled and empty states in these bands depends on both the defect density and on the position of the Fermi level. Therefore, the luminescence features and the residual absorption in the infrared are affected by annealing experiments that annihilate quenched-in defect pairs and change the position of the Fermi level due to changes in the native point defect chemistry. The latter has been tested by us using crystals grown by high pressure physical vapor transport in a dense phosphorus vapor atmosphere (HPVT), which allows the variation of the composition across the entire homogeneity range. Although it is the only method thus far that achieves n -type behavior in nominally undoped ZnGeP_2 crystals, it operates above the order-disorder temperature of ZnGeP_2 and is thus subject to the same limitations as melt growth experiments with regard to quenched-in nonequilibrium populations of antisite defects on the cation sublattice.

As to whether or not the problem of native defect control is solvable under low temperature vapor growth conditions is not known. Clearly quenched-in disorder on the cation sublattice should present less of a problem, but the low-sticking coefficients of P and Zn as compared to Ge favors the incorporation of excess Ge on P- and Zn-antisite positions even at high Zn:Ge and P:metal flow rate ratios. Thus low resistivity p -type material is obtained that is not suitable for the most interesting device applications. Nevertheless, stoichiometric heteroepitaxial films of excellent surface morphology and low concentrations of extrinsic point defects have been made, and the net carrier concentration decreases significantly with increasing silicon content in epitaxial $\text{ZnSi}_x\text{Ge}_{1-x}\text{P}_2$. Therefore, further improvements in the control of the electrical properties may be expected from future research.

V. SUMMARY

In conclusion, we propose a strategy for the heteroepitaxial overgrowth of silicon by compound semiconductors that separates the problems associated by interfacial chemistry and structure from the problems associated with the lattice mismatch. Of the mixed compound systems available $\text{Al}_x\text{Ga}_{1-x}\text{N}_y\text{P}_{1-y}$, $\text{ZnS}_y\text{Se}_{1-y}$ and $\text{ZnSi}_x\text{Ge}_{1-x}\text{P}_2$ are suitable candidates for exactly lattice-matched epitaxial overgrowth of silicon. Real-time process monitoring by nonintrusive methods is important for gaining an understanding of the epitaxial overgrowth mechanism and for controlling the film properties. A new method, p -polarized reflectance spectroscopy, is introduced that provides detailed information about the growth rate per cycle, the bulk optical properties of the film and its topography with submonolayer resolution for thousands of Å of film growth by pulsed chemical beam epitaxy. The most critical issue in the implementation of nearly lattice-matched overgrowth of silicon surfaces is the control of planar defect formation that is linked to residual surface contamination. Since very small levels of surface

contamination that are difficult to detect with existing methods of surface analysis suffice to result in substantial defect densities, research addressing this issue must take an empirical approach. Fortunately, PRS provides for the sensitive and immediate characterization of the deviations from a two-dimensional overgrowth, so that future empirical studies that relate the effects of modifications in the wafer cleaning, surface conditioning, precursor chemistry and pulse sequence to improvements in the overgrowth mechanism do not have to rely exclusively on time-consuming *ex situ* characterization experiments.

ACKNOWLEDGMENTS

This work has been supported by NASA Grant No. NAGW-2865, ARPA/AFOSR Grant No. F49620-94-1-047, and NSF Grant Nos. DMR-9202210 and CDR-8721505.

- ¹N. Mino, M. Kobayashi, M. Konagai, and K. Takahashi, *J. Appl. Phys.* **58**, 793 (1985).
²R. D. Bringans, D. K. Biegelsen, L.-E. Swartz, F. A. Ponce, and J. C. Tramontana, *Phys. Rev. B* **45**, 1340 (1992).
³Y. Takagi, T. Kawai, D. Saitoh, N. Ohshima, and K. Parkj, 1994 Electronic Materials Conf., Extended Abstracts paper V1, TMS Warrendale, PA.
⁴N. Dietz, A. Miller, and K. J. Bachmann, *J. Vac. Sci. Technol. B* **13**, 153 (1995).
⁵N. Dietz, A. Miller, J. T. Kelliher, D. Venables, and K. J. Bachmann,

- International Molecular-Beam Epitaxy Conference, Osaka, 1994 [*J. Cryst. Growth* (to be published)].
⁶J. T. Kelliher, N. Dietz, J. Thornton, G. Lucovsky, and K. J. Bachmann, *Mater. Sci. Eng. B* **22**, 97 (1993).
⁷J. W. Ornton, C. T. Foxon, T. S. Cheng, D. E. Lacklison, S. V. Novikov, D. Johnson, N. Baba-Ali, T. L. Tansley, S. Hooper, and L. J. Challis, 1994 Electronic Materials Conference, Extended Abstracts paper A35, TMS, Warrendale, PA (unpublished).
⁸G. B. Stringfellow, *J. Electrochem. Soc.* **119**, 1780 (1992).
⁹G. B. Stringfellow, *J. Cryst. Growth* **58**, 194 (1982).
¹⁰K. J. Bachmann, *Mater. Res. Soc. Symp. Proc.* **242**, 707 (1992).
¹¹N. Dietz and H. J. Lewerenz, *Appl. Surf. Sci.* **69**, 350 (1993).
¹²N. Kobayashi and Y. Hoshikawa, *Jpn. J. Appl. Phys.* **28**, L 1880 (1989).
¹³E. Kern, in *Current Topics of Materials Science*, edited by E. Kaldis (North-Holland, Amsterdam, 1979), Vol. 3, p. 131.
¹⁴J. T. Kelliher, J. T. Thornton, P. E. Russell, and K. J. Bachmann, *Mater. Res. Soc. Symp. Proc.* **317**, 597 (1994).
¹⁵R. J. Gillespie, *J. Chem. Educ.* **47**, 18 (1970).
¹⁶R. D. Bringans, D. K. Biegelsen, L. E. Swartz, F. A. Ponce, and J. C. Tramontana, *Appl. Phys. Lett.* **61**, 195 (1992).
¹⁷Y. Kohama, K. Uchida, T. Soga, T. Jimbo, and M. Umeno, *Appl. Phys. Lett.* **53**, 862 (1988).
¹⁸J. T. Kelliher, A. E. Miller, N. Dietz, S. Habermehl, Y. L. Chen, Z. Lu, G. Lucovsky, and K. J. Bachmann, *Appl. Surf. Sci.* **86**, 453 (1995).
¹⁹G. C. Xing, K. J. Bachmann, G. S. Solomon, J. B. Posthill, and M. L. Timmons, *J. Cryst. Growth* **94**, 381 (1989).
²⁰G. C. Xing, K. J. Bachmann, J. B. Posthill, and M. L. Timmons, *J. Appl. Phys.* **69**, 4286 (1991).
²¹N. Dietz, I. Tsveybak, W. Ruderman, G. Wood, and K. J. Bachmann, *Appl. Phys. Lett.* **65**, 2759 (1994).